Highest Wireless Power: Inductively Coupled Or RF?

Nan Xing, Graduate Student Member, IEEE, and Gabriel A. Rincón-Mora, Fellow, IEEE
Georgia Institute of Technology, Atlanta, Georgia 30332 U.S.A.
nxing3@gatech.edu and Rincon-Mora@gatech.edu

Abstract

Embedded microsensors are the critical components for the Internet of Things (IoT) as they provide interfaces between the physical and the digital worlds. Unfortunately, these microsensors' tiny batteries cannot sustain their operation for long. Ambient energy sources, such as light or motion, are not always available, so transmitting power wirelessly is often the only option to recharge their onboard batteries. This paper discusses and compares two of the most popular wireless power transfer technologies: inductively coupled and RF, in terms of their highest output power over distance. As an example, a 125 kHz, coil-based inductively coupled power transfer system is compared with a 2.45 GHz, antenna-based RF power transfer system. When closely coupled, the inductively coupled receiver outputs higher power density with a normalized transmitter. As the distance grows, the power density of the inductively coupled receiver decays 3 times faster than the RF. So past 3.5 times of the transmitter's length, the RF's power density beats the inductively coupled.

Keywords

Internet of things, embedded microsensor, wireless power transfer, inductively coupled, RF, maximum power.

1. Wireless power transfer

A. Embedded applications: implants etc.

Embedded microsensors technology has been a critical driving force for the IoT as it expands the IoT's territory by enabling more sensing capabilities in a non-obtrusive form. Embedded microsensors can be biomedical implants [1]–[2], structural health monitoring sensors [3]–[4], and environmental monitoring sensors [5]. However, the tiny batteries they contain onboard deplete quickly and need to be replenished from time to time. Harvesting ambient energy, such as light or motion, is tempting. However, such energy sources are rarely available in an embedded environment. Often, the only option left is to transfer power wirelessly.

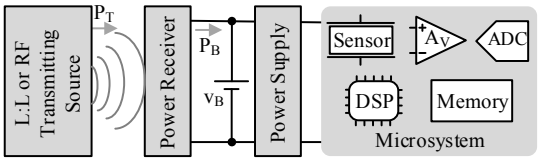

Fig. 1. Wireless powered embedded microsystem.

Transmitting power wirelessly over a long distance often involves using either a pair of inductively-coupled coils or RF antennas [6]–[7]. Although power can also be transferred via capacitive coupling, the power transmission distance is often as short as a few millimeters [8]. Fig. 1 shows a typical L-coupled/RF wireless system. The transmitter emits a magnetic/electromagnetic field into nearby space and sends out power P_T. The receiver captures the field and generates power P_B to charge up the battery v_B, which supplies system components, such as sensors, DSPs, etc.

B. Power density decay

As the transmitting source is not always available, the power receiver needs to charge up v_B with the highest power $P_{O(MAX)}$. Also, the power receiver's size needs to be small for the embedding purpose. Finally, the amount of transmitting power P_T is often limited by health and safety standards [9]. Therefore, with limited P_T, the best power receiver should generate the highest $P_{O(MAX)}$ from the smallest volume.

$$\eta_{PD} = \left(\frac{P_{O(MAX)}}{Vol_R}\right) \Big/ \left(\frac{P_{T(MAX)}}{Vol_T}\right) \quad (1)$$

The relative power density η_{PD}, as defined in (1), normalizes $P_{O(MAX)}$ with max transmitter power $P_{T(MAX)}$ and volume Vol_R. Therefore, η_{PD} can be used to assess the relative performance of the wireless power receiver when the transmitter size is the same. As Fig.2 shows, as the receiving coil/antenna separates further from the transmitting source, it captures a smaller portion of the field. So η_{PD} decays with distance d_X.

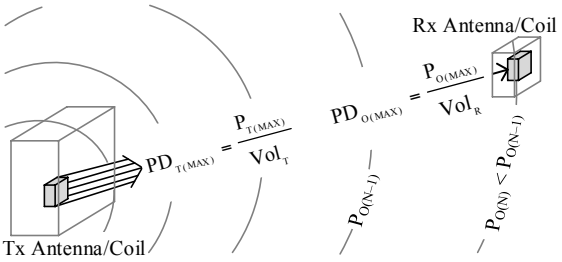

Fig. 2. Power density attenuation from the transmitter to the receiver

For the rest of the paper, Section II and III discuss the concept, system, and maximum output power of the L-coupled and RF power system, respectively. Section IV presents a case study that compares the performance of a 125 kHz L-coupled power system with a 2.45 GHz RF power system over distance. Relevant conclusions are drawn in Section V.

2. Inductively coupled

A. Concept

Inductively coupled power transfer utilizes a pair of coils to transfer power [6]. The transmitting coil L_T in Fig. 3 runs an AC current i_T and generates a changing magnetic field B_T in the nearby space. The receiving coil L_R captures the magnetic flux that L_T emits and induces an electromotive force (EMF) voltage v_E. From v_E the power receiver draws power and charges up v_B.

For most microsensor applications, the receiver coil's radius r_R is much smaller than the transmitter coil's radius r_T. With this premise, B_T along d_X direction is [10]:

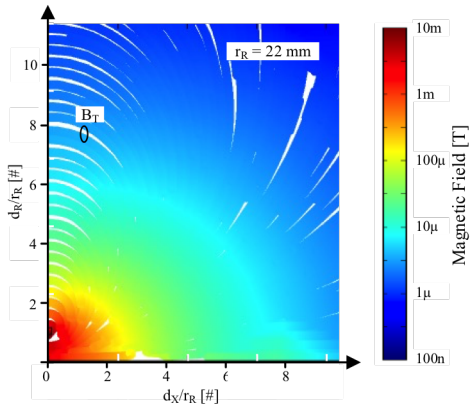

Fig. 4. FEM simulated cross-sectional magnetic field near the transmitting

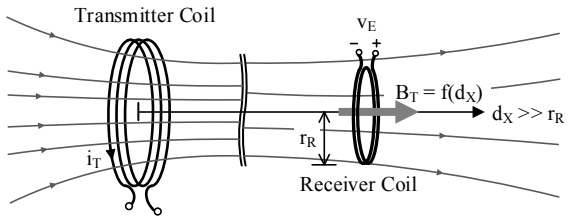

Fig. 3. Inductively coupled receiver coil generates an EMF voltage.

$$B_T = \left.\frac{0.5\mu_C N_T i_T r_T^{\,2}}{\left(r_T^{\,2} + d_X^{\,2}\right)^{1.5}}\right|_{d_X >> r_T} \propto \frac{1}{d_X^{\,3}}, \tag{2}$$

where N_T is the number of turns of the transmitter coil, and μ_C is the averaged permeability of the medium between the coils. B_T drops cubically with d_X when $d_X >> r_T$. When perfectly aligned, the induced v_E is proportional to the rate of captured magnetic flux change over time:

$$v_E = \frac{\partial\left(B_T A_R N_R\right)}{\partial t} \propto \left.\frac{\frac{di_T}{dt}}{\left(r_T^{\,2} + d_X^{\,2}\right)^{3/2}}\right|_{d_X >> r_T} \propto \frac{f_O}{d_X^{\,3}}, \tag{3}$$

where N_R and A_R are the number of turns and the area of the receiver coil. From (3), v_E also decays cubically with d_X.

To validate the B_T calculation in (2), the magnetic field generated by a 250-turn, 4.3 cm diameter coil is simulated using COMSOL Multiphysics. Fig. 4 shows the simulated B_T of a half cross-sectional plane that is perpendicular to the coil. The color in Fig. 4 represents B_T's magnitude while the lines show B_T's direction. The simulated B_T strength along the d_X axle is compared with the calculation in Fig. 5. When $d_X < 5.6\ d_T$, the calculation from (2) matches the simulated results within ±3% error. Beyond that, due to the dynamic range limit of the simulation, the error increases to ±10%.

B. Power transfer system

A typical L-coupled power transfer system is shown in Fig. 6. The power transmitter's L_T-C_T is usually driven by a power inverter [11]–[12] which is modeled by a low-impedance square-wave voltage source v_S. Since L_T-C_T only band-passes current at the resonant, the equivalent driving voltage at the transmitter is v_S' fundamental tone at f_O:

$$v_{S(PK)}^{\,(f_O)} = \left(\frac{4}{\pi}\right) v_{S(PK)}. \tag{4}$$

The current in L_T and couples an open-circuit voltage v_E on L_R. As the receiver draws more power from L_R, it loads the transmitter and reduces L_T's current, which in return lowers the closed-circuit coupled voltage $v_{E(CL)}$. This loading effect is modeled by the coupled impedance R_E [13]. The power that v_E-R_E avails is limited by the transmitting source, so:

$$P_{E(MAX)} = \frac{\left(\frac{0.5 v_{S(PK)}^{\,(f_O)}}{\sqrt{2}}\right)^2}{R_S + R_T} = \frac{\left(\frac{0.5 v_{E(PK)}}{\sqrt{2}}\right)^2}{R_E}. \tag{5}$$

From (5), the coupled resistance can be derived as:

$$R_E = \left(\frac{v_{E(PK)}}{\sqrt{2} v_{S(PK)}^{\,(f_O)}}\right)^2 \left(R_S + R_T\right). \tag{6}$$

The power receiver periodically re-direct the L_R's current to charge up v_B. Since R_R (L_R's equivalent series resistance (ESR)) and R_E's conduction loss dominates the receiver's power loss, $P_B \approx P_O$.

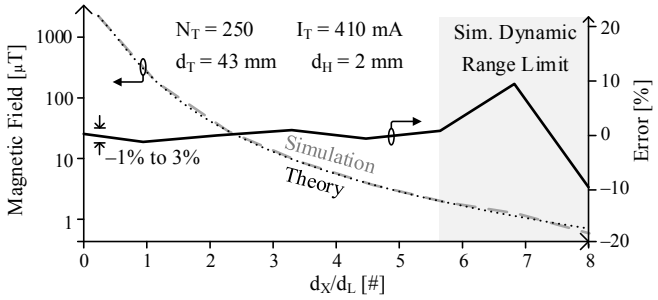

Fig. 5. Calculated and FEM simulated magnetic field along d_X.

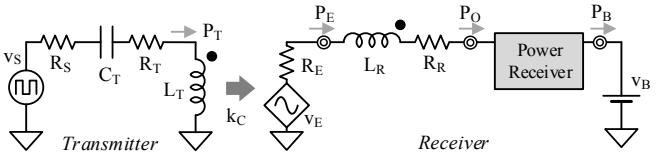

Fig. 6. Inductively coupled power transfer system.

C. Maximum output power

The key to drawing max power from L_R is that the receiver "load match" the source impedance [13], as Fig. 7 shows. A capacitor C_R is often used to create resonance and raise L_R's current, so as to boost the power drawn from v_E [13]. P_O is maximum when $v_R = 0.5\ v_E$ [14]:,

$$P_{O(MAX)} = \frac{\left(0.5 v_{E(RMS)}\right)^2}{R_E + R_R} = \frac{\left(\frac{0.5 v_{E(PK)}}{\sqrt{2}}\right)^2}{R_E + R_R}. \tag{7}$$

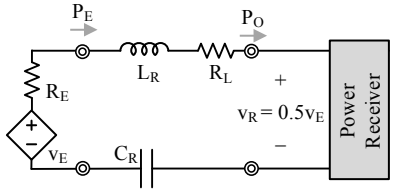

Fig. 7. Power model of the inductively coupled power receiver.

When closely coupled, $R_E >> R_R$. So $P_{O(MAX)} \approx P_{E(MAX)}$ and does not scale with d_X:

$$P_{O(MAX)}\Big|_{R_E >> R_R} \approx P_{E(MAX)} = \frac{\left(0.5 v_{S(PK)}^{\,(f_O)}\right)^2}{2R_T} \neq f\left(d_X\right). \tag{8}$$

At high d_X, the receiver barely loads the transmitter, so $R_E << R_R$. As a result, $P_{O(MAX)}$ scales quadratically with $v_{E(PK)}$:

$$P_{O(MAX)}\Big|_{R_R >> R_E} \approx \frac{\left(\frac{0.5v_{E(PK)}}{\sqrt{2}}\right)^2}{R_E} \propto \left(\frac{1}{d_X^3}\right)^2. \quad (9)$$

To validate the theory above, Fig. 8 compares the Spice simulated $P_{O(MAX)}$ with the calculation when the coupling k_C ranges from 0.01%-100%. Proportional to $v_{E(PK)}$ [6], k_C also drops cubically with d_X. The simulation adjusts the effective receiver load as a resistor in Fig. 6 for $P_{O(MAX)}$. The simulated $P_{O(MAX)}$ closely matches the theory's prediction. Below $k_{C(SAT)}$ (~1.5%), $P_{O(MAX)}$ drops –20dB/dec with $v_{E(PK)}$. Beyond $k_{C(SAT)}$ $P_{O(MAX)}$ saturates as the power is limited by the available power from the transmitter. The simulation matches the calculation within 0.1% to 0.2% error when $v_{E(PK)}$ is above 20 mV. Below 20 mV, the error increases to –0.4% to 2.5% due to the dynamic range limitation of the simulation.

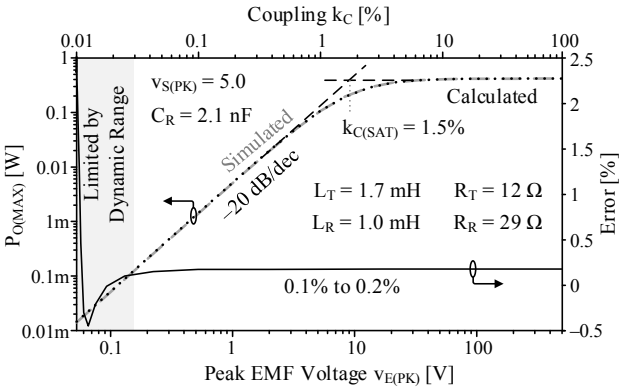

Fig. 8. Calculated and circuit simulated $P_{O(MAX)}$ at different $v_{E(PK)}$.

3. RF

A. Concept

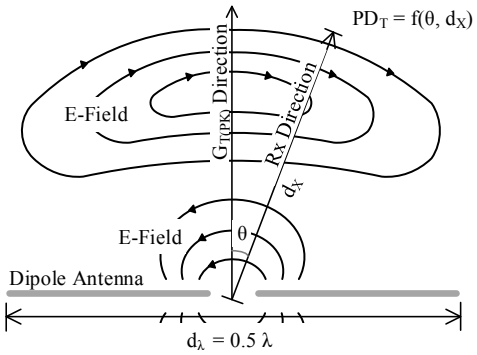

Fig. 9. Dipole antenna momentary electric field.

An RF antenna projects its power P_T to a sphere surface A_T, as Fig. 9 shows. For a non-isotropic antenna, the power radiation is not uniform in every direction. Antenna gain G_T characterizes the non-uniformity of power density in different directions. So the power density at d_X is both a function of d_X and angle θ, as Fig. 9 shows:

$$PD_T = \frac{P_T G_T}{A_T} = \frac{P_T G_T}{4\pi d_X^2}. \quad (10)$$

For dipole antennae, PD_T maximizes at θ = 0 and minimizes at θ = ±90°. The received power is proportional to both of PD_T, the effective receiver antenna aperture A_R', and the receiver's antenna gain G_R [15]:

$$P_O\Big|_{d_X > 4d_\lambda} = PD_T A_R' G_R = \left(\frac{P_T G_T}{4\pi d_X^2}\right)\left(\frac{d_\lambda^2}{\pi}\right) G_R. \quad (11)$$

Equation (11) is widely referred to as the Friis formula. Note the formula is reasonably accurate in the far-field region when $d_X > 4d_\lambda$, where d_λ is the length of the half-wave dipole antenna.

B. Power transfer system

In an RF system, a power amplifier drives the transmitting antenna that radiates P_T, as Fig. 10 shows. The receiver captures a fraction of P_T. A matching network minimizes the reflection power on the receiving antenna, so P_O is maximum. The current from the receiving antenna is rectified to charge v_B. A dedicated RF power transfer system does not require data communication blocks such as modulator, demodulator, or mixers.

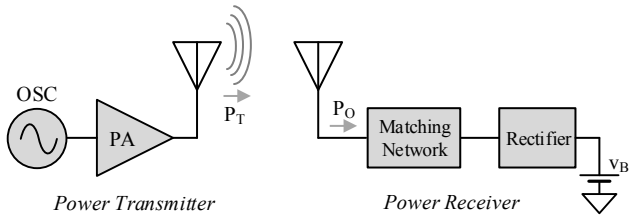

Fig. 10. RF power supply system

C. Maximum output power

The RF power transfer system generates the highest output power when both transmitter and receiver antennae align along their peak power density direction, so $P_{O(MAX)}$ drops quadratically with d_X:

$$P_{O(MAX)}\Big|_{d_X > 4d_\lambda} = P_T G_{T(PK)} \left(\frac{d_\lambda}{2\pi d_X}\right)^2 G_{R(PK)} \propto \frac{1}{d_X^2}. \quad (12)$$

$G_{T(PK)}$ of a dipole antenna is normally 2.15 dBi [16]. $G_{R(PK)}$ is the peak antenna gain of the receiver.

4. Inductively coupled vs. RF

A. Space constraints

Table I. Parameters for the inductively coupled and RF system

Parameter	Value	Parameter	Value
RF Power Receiver: TAOGLAS SWLP.2450.10.4.A.02			
d_H	4 mm	d_D	10 mm
d_L	10 mm	$G_{R(PK)}$	–1 dBi
L:L Power Transmitter Coil [17]			
μ_{EFF}	12.6 mN·A^{-2}	L_T	1.7 mH
N_T	250	R_T @ f_O	12.1 Ω
d_H	2 mm	f_O	125 kHz
r_T	21.5 mm	$v_{S(PK)}$	5 V
L:L Power Receiver Coil: Coilcraft 4513TC			
d_H	2.7 mm	L_R	1 mH
d_L	11.7 mm	$R_{ESR,R}$ @ f_O	23.9 Ω
d_D	3.5 mm	S_{RX}	31 mV/μT
RF Power Transmitter: Dipole [16]–[18]			
f_O	2.45 GHz	d_λ	61 mm
λ	122 mm	$G_{T(PK)}$	2.15 dBi

As an example, this section compares the power density decay of a 125 kHz L-coupled power system with a 2.45 GHz RF power system. While both 125 kHz and 13.56 MHz are widely used for L-coupled power transfer, 125 kHz operation

lowers the switching loss and is more suitable for low-power microsensor applications. 2.45 GHz is widely used for RF power transfer, so the power link can be shared with the data link such as Wifi and Bluetooth.

For a compact system, the transmitter needs to be small in all directions. The transmitter's dimension d_L characterizes the side length of the smallest square that the transmitter can fit into. A 2.45 GHz half-wave dipole measures 6.1 cm, which fits right into 4.3×4.3×0.2 cm^3 cubic of space, so its d_L is 4.3 cm. For a fair comparison, the L-coupled transmitter coil is also limited to the same cubic of space, as Fig. 11 shows. The inductor coil used here is a 250-turn, 43 mm diameter, single-row coil. The calculated inductance is around 1 mH [17].

For the receiver, the L-coupled power system uses the Coilcraft 4513TC 1 mH coil with 31 mV/μT sensitivity. The RF system uses the patch antenna SWLP.2450.10.4.A.02 from Taoglas. Fig. 12 shows their dimensions. Parameters of the transmitters and receivers are summarized in Table I.

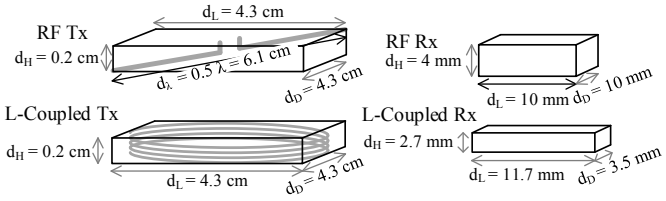

Fig. 11. Dimensions of the L-coupled and RF transmitters and receivers.

B. Power density decay

Fig. 13 compares the η_{PD} of the above discussed L-coupled and RF power transfer systems. The solid lines indicate the η_{PD} calculated from the theory, while the dashed line indicates the qualitatively projected η_{PD} of the RF system in the near-field region. The Friis equation (11) is only accurate for the far-field region. The power in the near-field region much more complex, as it is subject to the antenna's shape and position [19]. The discussion is beyond this paper's scope. Up to d_L, L-coupled system's η_{PD} stays flat, as the transmitting source limits $P_{O(MAX)}$. In this region, the L-coupled system's η_{PD} is always higher, as the L-coupled receiver can potentially source all the power that the transmitter avails, while the RF system always loses a portion of the power it radiates into space (% P_{LOSS}). Past d_L, $P_{O(MAX)}$ or η_{PD} drops 3 times faster than the RF system. Past 3.5 d_L, η_{PD} of the L-coupled system is surpassed by the RF system. More generally, RF system outputs higher power in the far-field region, while the inductively coupled system output higher power in deep near-field region.

5. Conclusions

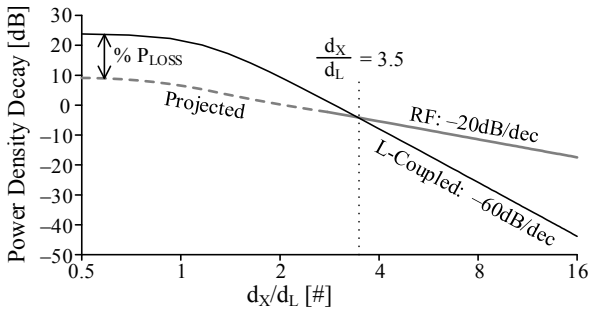

Fig. 13. Comparison between inductively coupled RF power density attenuation over distance.

This paper compares the maximum output power performance of the two most popular wireless power transfer technologies: L-coupled and RF. With normalized transmitter power and size, up to d_L, L-coupled power receiver outputs higher power density η_{PD}, as it can output as much power as the transmitter avails, while the RF system always loses the power that radiates into space. However, past d_L, the L-coupled system's η_{PD} decays 3 times as fast as the RF system over d_X. So beyond 3.5 d_L, RF's η_{PD} beats the L-coupled.

Acknowledgment

The authors thank Texas Instruments (TI) for sponsoring this research and Dr. Orlando Lazaro, Dr. Andres Blanco, and Dr. Jeff Morroni for their support and advice.

Reference

[1] H. Kassiri, A. Bagheri, *et al.*, "Battery-less tri-band-radio neuro-monitor and responsive neurostimulator for diagnostics and treatment of neurological disorders," *IEEE Journal of Solid-State Circuits,* vol. 51, no. 5, pp. 1274-89, 2016.

[2] Y. Zhang, F. Zhang, *et al.*, "A batteryless 19 w MICS/ISM-band energy harvesting body sensor node SoC for ExG applications," *IEEE Journal of Solid-State Circuits,* vol. 48, no. 1, pp. 199-213, 2013.

[3] A. Alvarez-Carulla, J. Colomer-Farrarons, *et al.*, "Piezoelectric harvester-based self-powered adaptive circuit with wireless data transmission capability for structural health monitoring," *IEEE Conference on Design of Circuits and Integrated Systems*, pp. 1-6, November, 2015

[4] M.J. Nothnagel, G. Park, *et al.*, "Wireless energy transmission for structural health monitoring embedded sensor nodes," *SPIE Health Monitoring of Structural and Biological Systems*, pp. 653216, 2007

[5] D. Cirmirakis, A. Demosthenous, *et al.*, "Humidity-to-frequency sensor in CMOS technology with wireless readout," *IEEE Sensors Journal,* vol. 13, no. 3, pp. 900-908, 2013.

[6] N. Xing, and G.A. Rincón-Mora, "180-nm 85%-efficient inductively coupled switched resonant half-bridge power receiver," *IEEE Transactions on Circuits and Systems II: Express Briefs,* vol. 66, no. 6, pp. 983-987, 2019.

[7] T. Umeda, H. Yoshida, *et al.*, "A 950-MHz rectifier circuit for sensor network tags with 10-m distance," *IEEE Journal of Solid-State Circuits,* vol. 41, no. 1, pp. 35-41, 2006.

[8] J. Dai, and D.C. Ludois, "A survey of wireless power transfer and a critical comparison of inductive and capacitive coupling for small gap applications," *IEEE Transactions on Power Electronics,* vol. 30, no. 11, pp. 6017-6029, 2015.

[9] "IEEE approved draft standard for safety levels with respect to human exposure to electric, magnetic and electromagnetic fields, 0 Hz to 300 GHz," *IEEE PC95.1/D3.5, October 2018,* pp. 1-312, 2019.

[10] Y. Lee, "RFID coil design," *Microchip Design Note,* no. AN678, 1998.

[11] U.K. Madawala, M. Neath, *et al.*, "A power–frequency controller for bidirectional inductive power transfer systems," *IEEE Transactions on Industrial Electronics,* vol. 60, no. 1, pp. 310-317, 2013.

[12] B.X. Nguyen, D.M. Vilathgamuwa, *et al.*, "An efficiency optimization scheme for bidirectional inductive power transfer systems," *IEEE Transactions on Power Electronics,* vol. 30, no. 11, pp. 6310-19, 2015.

[13] N. Xing, and G. Rincon-Mora, "Highest maximum power point of radially distant inductively coupled power receivers with deep submicron CMOS," *IEEE Transactions on Industrial Informatics,* DOI: 10.1109/TII.2019.2910092.

[14] C.S. Kong, "A general maximum power transfer theorem," *IEEE Transactions on Education,* vol. 38, no. 3, pp. 296-298, 1995.

[15] S. Keyrouz, H.J. Visser, *et al.*, "Ambient RF energy harvesting from DTV stations," *2012 Loughborough Antennas & Propagation Conference*, pp. 1-4, 2012

[16] K. Wei, Z. Zhang, *et al.*, "A triband shunt-fed omnidirectional planar dipole array," *IEEE Antennas and Wireless Propagation Letters,* vol. 9, pp. 850-853, 2010.

[17] M.J. Wilson, and S.R. Ford, *The ARRL Handbook for Radio Communications 2007*: American Radio Relay League, 2006.

[18] T. Yestrebsky, "MICRF001 Antenna Design Tutorial," *Application Note,* vol. 23, p. 8, 1999.
[19] A. Yaghjian, "An overview of near-field antenna measurements," *IEEE Transactions on Antennas and Propagation,* vol. 34, no. 1, pp. 30-45, 1986.